

# Chapter 7

## Fixed points

**S**O FAR WE HAVE LEARNED that periodic orbits offer invariant characterization of dynamics in two ways: (a) their existence and inter-relations are a topological, coordinate-independent property of the dynamics, and (b) their Floquet multipliers form an infinite set of *metric invariants*. Typically they are unstable and hard to find. But do we really need them? By chapter 18 you will understand that the answer is a resounding yes.

Sadly, searching for periodic orbits will never become as popular as a week on Côte d’Azur, or publishing yet another log-log plot in *Phys. Rev. Letters*. This chapter is one of four hands-on chapters on extraction of periodic orbits, and can be skipped on first reading - you can return to it whenever the need for finding actual cycles arises.



fast track:  
chapter 14, p. 358

A serious cyclist will ask “Where are the cycles? And what if they are long?” and read chapter 13. She will want to also learn about the variational methods which will enable her to find arbitrarily long, arbitrarily unstable cycles, and read chapter 33. So here is the key and unavoidable numerical task we must face up to: find “all(?)” solutions  $(x, T)$ ,  $x \in \mathbb{R}^d$ ,  $T \in \mathbb{R}$  satisfying the *periodic orbit condition*

chapter 13

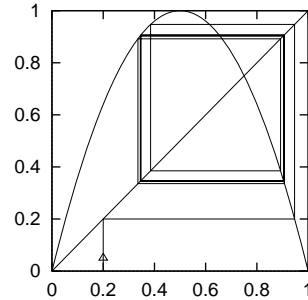
chapter 33

$$f^{t+T}(x) = f^t(x), \quad T > 0 \tag{7.1}$$

for a given flow or map.

A *prime cycle*  $p$  of period  $T_p$  is a single traversal of the periodic orbit, so our task will be to find a periodic point  $x \in \mathcal{M}_p$  and the shortest time  $T_p$  for which (7.1) has a solution. A periodic point of a flow  $f^t$  crossing a Poincaré section

**Figure 7.1:** The inverse time path to the  $\overline{01}$ -cycle of the logistic map  $f(x) = 4x(1-x)$  from an initial guess of  $x = 0.2$ . At each inverse iteration we chose the 0 (respectively 1) branch.



$n$  times is a fixed point of  $P^n$ , the  $n$ th iterate of  $P$ , the return map (3.1); hence, we shall refer to all cycles as “fixed points” in this chapter. By cyclic invariance, Floquet multipliers and the period of the cycle are independent of the choice of the initial point, so it will suffice to solve (7.1) at a single periodic point. section 5.3

If the cycle is an attracting limit cycle with a sizable basin of attraction, it can be found by integrating the flow for a sufficiently long time. If the cycle is unstable, simple integration forward in time will not reveal it, and the methods to be described here need to be deployed. In essence, any method for finding a cycle is based on devising a new dynamical system which possesses the same cycle, but for which this cycle is attractive. Beyond that, there is a great freedom in constructing such systems, and many different methods are used in practice.

## 7.1 One-dimensional maps

(F. Christiansen)

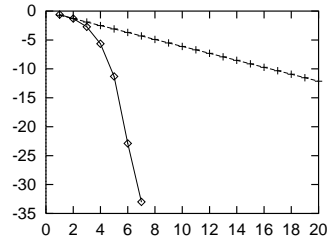
So far we have given some qualitative hints for how to set out on a periodic orbit hunt. In what follows, we teach you how to nail down periodic orbits numerically.

### 7.1.1 Inverse iteration

Let us first consider a very simple method to find the unstable cycles of a 1-dimensional map such as the logistic map. Unstable cycles of 1-dimensional maps are attracting cycles of the inverse map. The inverse map is not single-valued, so at each backward iteration we have a choice of branch to make. By choosing the branch according to the symbolic dynamics of the cycle we are trying to find, we will automatically converge to the desired cycle. The rate of convergence is given by the stability of the cycle, i.e., the convergence is exponentially fast. Figure 7.1 shows such a path to the  $\overline{01}$ -cycle of the logistic map. exercise 13.10

The method of inverse iteration is fine for finding cycles for 1-d maps and some 2-dimensional systems such as the repeller of exercise 13.10. It is not particularly fast, however, especially if the inverse map is not known analytically. It

**Figure 7.2:** Convergence of Newton method ( $\diamond$ ) vs. inverse iteration ( $+$ ). The error after  $n$  iterations searching for the  $\overline{01}$ -cycle of the logistic map  $f(x) = 4x(1-x)$  with an initial starting guess of  $x_1 = 0.2, x_2 = 0.8$ . The y-axis is  $\log_{10}$  of the error. The difference between the exponential convergence of the inverse iteration method and the super-exponential convergence of Newton method is dramatic.



also completely fails for higher dimensional systems where we have both stable and unstable directions. Inverse iteration will exchange these, but we will still be left with both stable and unstable directions. The best strategy is to directly attack the problem of finding solutions of  $f^T(x) = x$ .

### 7.1.2 Newton method

Newton method for determining a zero  $x^*$  of a function  $F(x)$  of one variable is based on a linearization around a starting guess  $x_0$ :

$$F(x) \approx F(x^{(0)}) + F'(x^{(0)})(x - x^{(0)}). \tag{7.2}$$

An approximate solution  $x^{(1)}$  of  $F(x) = 0$  is

$$x^{(1)} = x^{(0)} - F(x^{(0)})/F'(x^{(0)}). \tag{7.3}$$

The approximate solution can then be used as a new starting guess in an iterative process. A fixed point of a map  $f$  is a solution to  $F(x) = x - f(x) = 0$ . We determine  $x$  by iterating

$$\begin{aligned} x^{(m)} &= g(x^{(m-1)}) = x^{(m-1)} - F(x^{(m-1)})/F'(x^{(m-1)}) \\ &= x^{(m-1)} - \frac{1}{1 - f'(x^{(m-1)})}(x^{(m-1)} - f(x^{(m-1)})). \end{aligned} \tag{7.4}$$

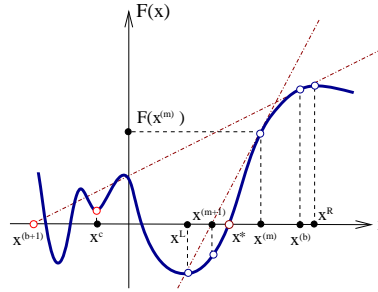
Provided that the fixed point is not marginally stable,  $f'(x) \neq 1$  at the fixed point  $x$ , a fixed point of  $f$  is a super-stable fixed point of the Newton-Raphson map  $g$ ,  $g'(x) = 0$ , and with a sufficiently good initial guess, the Newton-Raphson iteration will converge super-exponentially fast.

To illustrate the efficiency of Newton method we compare it to the inverse iteration method in figure 7.2. Newton method wins hands down: the number of significant digits of the accuracy of the  $x$  estimate typically doubles with each iteration.

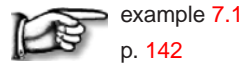
In order to avoid jumping too far from the desired  $x^*$  (see figure 7.3), one often initiates the search by the *damped Newton method*,

$$\Delta x^{(m)} = x^{(m+1)} - x^{(m)} = -\frac{F(x^{(m)})}{F'(x^{(m)})} \Delta \tau, \quad 0 < \Delta \tau \leq 1,$$

**Figure 7.3:** Newton method: bad initial guess  $x^{(b)}$  leads to the Newton estimate  $x^{(b+1)}$  far away from the desired zero of  $F(x)$ . Sequence  $\dots, x^{(m)}, x^{(m+1)}, \dots$ , starting with a good guess converges super-exponentially to  $x^*$ . The method diverges if it iterates into the basin of attraction of a local minimum  $x^c$ .



takes small  $\Delta\tau$  steps at the beginning, reinstating to the full  $\Delta\tau = 1$  jumps only when sufficiently close to the desired  $x^*$ .



example 7.1  
p. 142

## 7.2 Flows

(R. Paškauskas and P. Cvitanović)

For a continuous time flow the periodic orbit the Floquet multiplier (5.13) along the flow direction always equals unity; the separation of any two points along a cycle remains unchanged after a completion of the cycle. More unit Floquet multipliers arise if the flow satisfies conservation laws, such as the symplectic invariance for Hamiltonian flows, or the dynamics is equivariant under a continuous symmetry transformation.

section 5.3.1

section 10.3

Let us apply the Newton method of (7.3) to search for periodic orbits with unit Floquet multipliers, starting with the case of a *continuous time flow*. Assume that the periodic orbit condition (7.1) holds for  $x + \Delta x$  and  $T + \Delta t$ , with the initial guesses  $x$  and  $T$  close to the desired solution, i.e., with  $|\Delta x|, \Delta t$  small. The Newton setup (7.3)

$$\begin{aligned} 0 &= x + \Delta x - f^{T+\Delta t}(x + \Delta x) \\ &\approx x - f^T(x) + (1 - J(x)) \cdot \Delta x - v(f^T(x))\Delta t \end{aligned} \tag{7.5}$$

suffers from two shortcomings. First, we now need to solve not only for the periodic point  $x$ , but for the period  $T$  as well. Second, the marginal, unit Floquet multiplier (5.13) along the flow direction (arising from the time-translation invariance of a periodic orbit) renders the factor  $(1 - J)$  in (7.4) non-invertible: if  $x$  is close to the solution,  $f^T(x) \approx x$ , then  $J(x) \cdot v(x) = v(f^T(x)) \approx v(x)$ . If  $\Delta x$  is parallel to the velocity vector, the derivative term  $(1 - J) \cdot \Delta x \approx 0$ , and it becomes harder to invert  $(1 - J)$  as the iterations approach the solution.

As a periodic orbit  $p$  is a 1-dimensional set of points invariant under dynamics, Newton guess is not improved by picking  $\Delta x$  such that the new point lies on the

orbit of the initial one, so we need to constrain the variation  $\Delta x$  to directions transverse to the flow, by requiring, for example, that

$$v(x) \cdot \Delta x = 0. \quad (7.6)$$

Combining this constraint with the variational condition (7.5) we obtain a Newton setup for flows, best displayed in the matrix form:

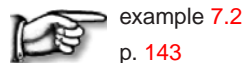
$$\begin{pmatrix} 1 - J(x) & -v(x) \\ v(x) & 0 \end{pmatrix} \begin{pmatrix} \Delta x \\ \Delta t \end{pmatrix} = - \begin{pmatrix} x - f(x) \\ 0 \end{pmatrix} \quad (7.7)$$

This illustrates the general strategy for determining periodic orbits in presence of continuous symmetries - for each symmetry, pick a point on the orbit by imposing a constraint, and compute the value of the corresponding continuous parameter (here the period  $T$ ) by iterating the enlarged set of Newton equations. Constraining the variations to transverse ones thus fixes both of Newton's shortcomings: it breaks the time-translation invariance, and the period  $T$  can be read off once the fixed point has been found (hence we omit the superscript in  $f^T$  for the remainder of this discussion).

More generally, the Poincaré surface of section technique of sect. 3.1 turns the periodic orbit search into a fixed point search on a suitably defined surface of section, with a neighboring point variation  $\Delta x$  with respect to a reference point  $x$  constrained to *stay* on the surface manifold (3.2),

$$U(x + \Delta x) = U(x) = 0. \quad (7.8)$$

The price to pay are constraints imposed by the section: in order to *stay* on the surface, arbitrary variation  $\Delta x$  is not allowed.



example 7.2  
p. 143

## Résumé

There is no general computational algorithm that is guaranteed to find all solutions (up to a given period  $T_{max}$ ) to the periodic orbit condition

$$f^{t+T}(x) = f^t(x), \quad T > 0$$

for a general flow or mapping. Due to the exponential divergence of nearby trajectories in chaotic dynamical systems, direct solution of the periodic orbit condition

can be numerically very unstable. With a sufficiently good initial guess for a point  $x$  on the cycle, however, the Newton-Raphson formula

$$\begin{pmatrix} 1 - J & -v(x) \\ a & 0 \end{pmatrix} \begin{pmatrix} \delta x \\ \delta T \end{pmatrix} = \begin{pmatrix} f(x) - x \\ 0 \end{pmatrix}$$

yields improved estimate  $x' = x + \delta x, T' = T + \delta T$ . Newton-Raphson iteration then yields the period  $T$  and the location of a periodic point  $x_p$  in the Poincaré section  $(x_p - x_0) \cdot a = 0$ , where  $a$  is a vector normal to the Poincaré section at  $x_0$ .

### Commentary

**Remark 7.1** Piecewise linear maps. The Lozi map (3.19) is linear, and hundred of thousands of cycles can easily be computed by [2x2] matrix multiplication and inversion.

**Remark 7.2** Newton gone wild. Skowronek and Gora [22] offer an interesting discussion of Newton iterations gone wild while searching for roots of polynomials as simple as  $x^2 + 1 = 0$ .

### 7.3 Examples

**Example 7.1 Rössler attractor.** We run a long simulation of the Rössler flow  $f^t$ , plot a Poincaré section, as in figure 3.2, and extract the corresponding Poincaré return map  $P$ , as in figure 3.3. Luck is with us, since figure 7.4(a) return map  $y \rightarrow P_1(y, z)$  is quite reminiscent of a parabola, we take the unimodal map symbolic dynamics, sect. 11.3, as our guess for the covering dynamics. Strictly speaking, the attractor is “fractal,” but for all practical purposes the return map is 1-dimensional; your printer will need a resolution better than  $10^{14}$  dots per inch to even begin resolving its structure.

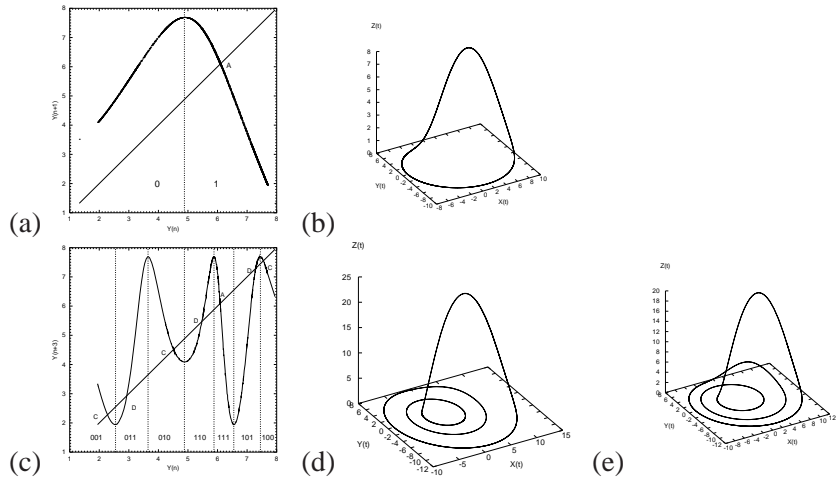
Periodic points of a prime cycle  $p$  of cycle length  $n_p$  for the  $x = 0, y > 0$  Poincaré section of the Rössler flow figure 2.6 are fixed points  $(y, z) = P^{n_p}(y, z)$  of the  $n$ th Poincaré return map.

Using the fixed point  $y_{k+1} = y_k$  in figure 7.4(a) together with the simultaneous fixed point of the  $z \rightarrow P_1(y, z)$  return map (not shown) as a starting guess  $(0, y^{(0)}, z^{(0)})$  for the Newton-Raphson search for the cycle  $p$  with symbolic dynamics label  $\bar{1}$ , we find the cycle figure 7.4(b) with the Poincaré section point  $(0, y_p, z_p)$ , period  $T_p$ , expanding, marginal, contracting Floquet multipliers  $(\Lambda_{p,e}, \Lambda_{p,m}, \Lambda_{p,c})$ , and the corresponding Lyapunov exponents  $(\lambda_{p,e}, \lambda_{p,m}, \lambda_{p,c})$ :

exercise 13.7

$$\begin{aligned} \bar{1}\text{-cycle:} \quad (x, y, z) &= (0, 6.09176832, 1.2997319) \\ T_1 &= 5.88108845586 \\ (\Lambda_{1,e}, \Lambda_{1,m}, \Lambda_{1,c}) &= (-2.40395353, 1 + 10^{-14}, -1.29 \times 10^{-14}) \\ (\lambda_{1,e}, \lambda_{1,m}, \lambda_{1,c}) &= (0.149141556, 10^{-14}, -5.44). \end{aligned} \tag{7.9}$$

**Figure 7.4:** (a) The  $y \rightarrow P_1(y, z)$  return map for the  $x = 0, y > 0$  Poincaré section of the Rössler flow figure 2.6. (b) The  $\overline{1}$ -cycle found by taking the fixed point  $y_{k+n} = y_k$  together with the fixed point of the  $z \rightarrow z$  return map (not shown) as an initial guess  $(0, y^{(0)}, z^{(0)})$  for the Newton-Raphson search. (c) The third iterate,  $y_{k+3} = P_1^3(y_k, z_k)$ , of the Poincaré return map (3.1) together with the corresponding plot for  $z_{k+3} = P_2^3(y_k, z_k)$ , is used to pick initial guesses for the Newton-Raphson searches for the two 3-cycles: (d) the  $\overline{001}$  cycle, and (e) the  $\overline{011}$  cycle. (G. Simon)



The Newton-Raphson method that we used is described in sect. 7.2.

As an example of a search for longer cycles, we use  $y_{k+3} = P_1^3(y_k, z_k)$ , the third iterate of the Poincaré return map (3.1) plotted in figure 7.4 (c), together with a corresponding plot for  $z_{k+3} = P_2^3(y_k, z_k)$ , to pick starting guesses for the Newton-Raphson searches for the two 3-cycles plotted in figure 7.4 (d), (e). For a listing of the short cycles of the Rössler flow, consult exercise 13.7.

The numerical evidence suggests (though a proof is lacking) that all cycles that comprise the strange attractor of the Rössler flow are hyperbolic, each with an expanding eigenvalue  $|\Lambda_e| > 1$ , a contracting eigenvalue  $|\Lambda_c| < 1$ , and a marginal eigenvalue  $|\Lambda_m| = 1$  corresponding to displacements along the direction of the flow.

For the Rössler flow the contracting eigenvalues turn out to be insanely contracting, a factor of  $e^{-32}$  per one par-course of the attractor, so their numerical determination is quite difficult. Fortunately, they are irrelevant; for all practical purposes the strange attractor of the Rössler flow is 1-dimensional, a very good realization of a horseshoe template. (G. Simon and P. Cvitanović)

[click to return: p. 140](#)

**Example 7.2 A hyperplane Poincaré section.** Let us for the sake of simplicity assume that the Poincaré surface of section is a (hyper)-plane, i.e., it is given by the linear condition (3.14)

$$(x - x_0) \cdot \hat{n} = 0, \tag{7.10}$$

where  $\hat{n}$  is a vector normal to the Poincaré section and  $x_0$  is any point in the Poincaré section. The Newton setup is then (derived as (7.7))

$$\begin{pmatrix} 1 - J & -v(x) \\ \hat{n} & 0 \end{pmatrix} \begin{pmatrix} x' - x \\ \Delta t \end{pmatrix} = \begin{pmatrix} -F(x) \\ 0 \end{pmatrix}. \tag{7.11}$$

The last row in this equation ensures that  $x$  will be in the surface of section, and the addition of  $v(x)\Delta t$ , a small vector along the direction of the flow, ensures that such an  $x$  can be found, at least if  $x$  is sufficiently close to a fixed point of  $f$ . Alternatively, this can be solved a least squares problem.

To illustrate that the addition of the extra constraint resolves the problem of  $(1 - J)$  non-invertability, we consider the particularly simple example of a 3-d flow with the  $(x, y, 0)$ -plane as the Poincaré section,  $a = (0, 0, 1)$ . Let all trajectories cross the

Poincaré section perpendicularly, so that  $v = (0, 0, v_z)$ , which means that the marginally stable direction is also perpendicular to the Poincaré section. Furthermore, let the unstable direction be parallel to the  $x$ -axis and the stable direction be parallel to the  $y$ -axis. The Newton setup is now

$$\begin{pmatrix} 1 - \Lambda_u & 0 & 0 & 0 \\ 0 & 1 - \Lambda_s & 0 & 0 \\ 0 & 0 & 0 & -v_z \\ 0 & 0 & 1 & 0 \end{pmatrix} \begin{pmatrix} \delta_x \\ \delta_y \\ \delta_z \\ \delta\tau \end{pmatrix} = \begin{pmatrix} -F_x \\ -F_y \\ -F_z \\ 0 \end{pmatrix}. \quad (7.12)$$

If one considers only the upper-left  $[3 \times 3]$  matrix (which we started out with, prior to adding the constraint (7.10)) then this matrix is not invertible and the equation does not have a unique solution. However, the full  $[4 \times 4]$  matrix is invertible, as  $\det(\cdot) = -v_z \det(1 - M_\perp)$ , where  $M_\perp$  is the  $[2 \times 2]$  monodromy matrix for a surface of section transverse to the orbit (see sect. 5.5).  
(F. Christiansen)

[click to return: p. 141](#)

## Exercises

- 7.1. **Rössler flow cycles.** (continuation of exercise 4.5) Determine all cycles for the Rössler flow (2.23), as well as their stabilities, up to 3 Poincaré section returns.

**Table:** The Rössler flow (2.23): The itinerary  $p$ , a periodic point  $x_p = (0, y_p, z_p)$  and the expanding eigenvalue  $\Lambda_p$  for cycles up to topological length 3.

(J. Mathiesen, G. Simon, A. Basu)

$n_p$	$p$	$y_p$	$z_p$	$\Lambda_e$
1	1	6.091768	1.299732	-2.403953
2	01	3.915804	3.692833	-3.512007
3	001	2.278281	7.416481	-2.341923
	011	2.932877	5.670806	5.344908

- 7.2. **Inverse iteration method for a Hénon repeller.**

**Table:** All periodic orbits up to 6 bounces for the Hamiltonian Hénon map (7.13) with  $a = 6$ . Listed are the cycle itinerary, its expanding eigenvalue  $\Lambda_p$ , and its “center of mass.” The “center of mass” is listed because it turns out that it is often a simple rational or a quadratic irrational.

$p$	$\Lambda_p$	$\sum x_{p,i}$
0	$0.715168 \times 10^1$	-0.607625
1	$-0.295285 \times 10^1$	0.274292
10	$-0.989898 \times 10^1$	0.333333
100	$-0.131907 \times 10^3$	-0.206011
110	$0.558970 \times 10^2$	0.539345
1000	$-0.104430 \times 10^4$	-0.816497
1100	$0.577998 \times 10^4$	0.000000
1110	$-0.103688 \times 10^3$	0.816497
10000	$-0.760653 \times 10^4$	-1.426032
11000	$0.444552 \times 10^4$	-0.606654
10100	$0.770202 \times 10^3$	0.151375
11100	$-0.710688 \times 10^3$	0.248463
11010	$-0.589499 \times 10^3$	0.870695
11110	$0.390994 \times 10^3$	1.095485
100000	$-0.545745 \times 10^5$	-2.034134
110000	$0.322221 \times 10^5$	-1.215250
101000	$0.513762 \times 10^4$	-0.450662
1111000	$-0.478461 \times 10^4$	-0.366025
110100	$-0.639400 \times 10^4$	0.333333
101100	$-0.639400 \times 10^4$	0.333333
111100	$0.390194 \times 10^4$	0.548583
111010	$0.109491 \times 10^4$	1.151463
111110	$-0.104338 \times 10^4$	1.366025

Consider the Hénon map (3.17) for the area-preserving (“Hamiltonian”) parameter value  $b = -1$ . The coordinates of a periodic orbit of length  $n_p$  satisfy the equation

$$x_{p,i+1} + x_{p,i-1} = 1 - ax_{p,i}^2, \quad i = 1, \dots, n_p, \quad (7.13)$$

with the periodic boundary condition  $x_{p,0} = x_{p,n_p}$ . Verify that the itineraries and the stabilities of the short periodic orbits for the Hénon repeller (7.13) at  $a = 6$  are as listed above.

**Hint:** you can use any cycle-searching routine you wish, but for the complete repeller case (all binary sequences are realized), the cycles can be evaluated simply by inverse iteration, using the inverse of (7.13)

$$x''_{p,i} = S_{p,i} \sqrt{\frac{1 - x'_{p,i+1} - x'_{p,i-1}}{a}}, \quad i = 1, \dots, n_p.$$

Here  $S_{p,i}$  are the signs of the corresponding periodic point coordinates,  $S_{p,i} = x_{p,i}/|x_{p,i}|$ . (G. Vattay)

- 7.3. **“Center of mass” puzzle\*\*.** Why is the “center of mass,” tabulated in exercise 7.2, often a rational number?
- 7.4. **Cycle stability, helium.** Add to the helium integrator of exercise 2.10 a routine that evaluates the expanding eigenvalue for a given cycle.

## References

- [7.1] D. Auerbach, P. Cvitanović, J.-P. Eckmann, G.H. Gunaratne and I. Procaccia, *Phys. Rev. Lett.* **58**, 2387 (1987).
- [7.2] M. Baranger and K.T.R. Davies *Ann. Physics* **177**, 330 (1987).
- [7.3] B.D. Mestel and I. Percival, *Physica D* **24**, 172 (1987); Q. Chen, J.D. Meiss and I. Percival, *Physica D* **29**, 143 (1987).
- [7.4] find Helleman et all Fourier series methods
- [7.5] J.M. Greene, *J. Math. Phys.* **20**, 1183 (1979)
- [7.6] P.H. Richter, H.-J. Scholz and A. Wittek, “A breathing chaos,” *Nonlinearity* **1**, 45 (1990).
- [7.7] H.E. Nusse and J. Yorke, “A procedure for finding numerical trajectories on chaotic saddles” *Physica D* **36**, 137 (1989).
- [7.8] D.P. Lathrop and E.J. Kostelich, “Characterization of an experimental strange attractor by periodic orbits” *Phys. Rev. A* **40**, 4028 (1989).
- [7.9] T. E. Huston, K.T.R. Davies and M. Baranger *Chaos* **2**, 215 (1991).
- [7.10] M. Brack, R. K. Bhaduri, J. Law and M. V. N. Murthy, *Phys. Rev. Lett.* **70**, 568 (1993).
- [7.11] C. Polymilis, G. Servizi, Ch. Skokos, G. Turchetti, and M. N. Vrahatis, “Locating periodic orbits by Topological Degree theory;” [arXiv:nlin.CD/0211044](https://arxiv.org/abs/nlin.CD/0211044).
- [7.12] B. Doyon and L. J. Dubé, “On Jacobian matrices for flows,” *CHAOS* **15**, 013108 (2005).
- [7.13] S.C. Farantos, “Exploring Molecular Vibrational Motions with Periodic Orbits,” *Int. Rev. Phys. Chem.* **15**, 345 (1996);  
[tccc.iesl.forth.gr/~farantos](http://tccc.iesl.forth.gr/~farantos),  
[tccc.iesl.forth.gr/articles/review/review1.ps.gz](http://tccc.iesl.forth.gr/articles/review/review1.ps.gz).
- [7.14] S.C. Farantos, “POMULT: A Program for Computing Periodic Orbits in Hamiltonian Systems Based on Multiple Shooting Algorithms,” *Computer Phys. Comm.* **108**, 240 (1998);  
[esperia.iesl.forth.gr/~farantos/articles/po\\_cpc/po\\_ccp.ps](http://esperia.iesl.forth.gr/~farantos/articles/po_cpc/po_ccp.ps).
- [7.15] M. Baranger, K.T.R. Davies and J.H. Mahoney, “The calculation of periodic trajectories,” *Ann. Phys.* **186**, 95 (1988).
- [7.16] K.T.R. Davies, T.E. Huston and M. Baranger, “Calculations of periodic trajectories for the Henon-Heiles Hamiltonian using the monodromy method,” *CHAOS* **2**, 215 (1992).
- [7.17] N.S. Simonović, “Calculations of periodic orbits: The monodromy method and application to regularized systems,” *CHAOS* **9**, 854 (1999).

- [7.18] N.S. Simonović, “Calculations of Periodic Orbits for Hamiltonian Systems with Regularizable Singularities,” *Few-Body-Systems* **32**, 183 (2003).
- [7.19] Z. Gills, C. Iwata, R. Roy, I.B. Schwartz and I. Triandaf, “Tracking Unstable Steady States: Extending the Stability Regime of a Multimode Laser System,” *Phys. Rev. Lett.* **69**, 3169 (1992).
- [7.20] N.J. Balmforth, P. Cvitanović, G.R. Ierley, E.A. Spiegel and G. Vattay, “Advection of vector fields by chaotic flows,” *Stochastic Processes in Astrophysics, Annals of New York Academy of Sciences* **706**, 148 (1993); [preprint](#).
- [7.21] A. Endler and J.A.C. Gallas, “Rational reductions of sums of orbital coordinates for a Hamiltonian repeller,” (2005).
- [7.22] L. Skowronek and P. F. Gora, “Chaos in Newtonian iterations: Searching for zeros which are not there,” *Acta Phys. Polonica B* **38**, 1909 (2007); [arXiv:nlin.CD/0703061](#).